ACS Photonics

Article

pubs.acs.org/journal/apchd5

Athermal and High-Q Hybrid TiO_2–Si_3N_4 Ring Resonator via an Etching-Free Fabrication Technique

Feng Qiu, Andrew M. Spring, and Shiyoshi Yokoyama*

Institute for Materials Chemistry and Engineering, Kyushu University, 6-1 Kasuga-koen Kasuga-city, Fukuoka, 816-8580, Japan

ABSTRACT: In this work, we have demonstrated a hybrid TiO_2–Si_3N_4 ring resonator with a high-Q and a temperature-insensitive resonance. The waveguide consists of a thermo-optic positive Si_3N_4 slab and a negative TiO_2 overcladding. The TiO_2 layer has a shallow ridge structure, which has been designed to realize an athermal operation and maintain a low scattering loss. During the fabrication of this waveguide, there was no need to utilize the dry-etching process. The method affords a straightforward fabrication and a precise control over the waveguide dimensions. As a result, the ring resonator exhibits a high Q value of 1.55×10^5, a low propagation loss of 0.4 dB/cm, and a small temperature-dependent wavelength shift of 0.14 pm/°C between 25 and 60 °C.

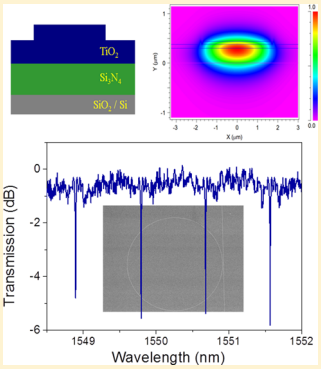

KEYWORDS: *waveguide, ring resonator, athermal*

High-Q ring resonators are a crucial component in various optical devices, such as frequency combs, sensors, electro-optic modulators and so on.[1−6] Of the various materials available for fabricating a resonator-on-a-chip, Si_3N_4 has been recently utilized in integrated optical devices because of its wide transparent window ranging from the visible to infrared wavelengths as well as its high refractive index of ∼2.0 enabling a strong confinement of the optical mode. Additionally, Si_3N_4 has a high Kerr nonlinearity but a low two photon and free carrier absorption at 1550 nm, which is preferred for the parametric oscillation application.[1,7] However, one problem of high-Q ring resonators in practical applications is a remarkable temperature sensitivity due to the materials' thermo-optic coefficient (TOC). Actually, Si_3N_4 has a TOC of 4×10^{-5}/°C, which means that the temperature drift results in a variation of the Si_3N_4 refractive index.[8] This refractive index variation induces a change in the effective index and propagation constant of the waveguide, and thus significantly disrupts the designed phase relation in a ring resonator. In fact, Si_3N_4 ring resonators with a Q-factor of 3×10^4 tunes out of its resonance (transmission change > 3 dB) with only 1 °C change in temperature. Clearly, it is desirable to realize an athermal operation for the optimized application of Si_3N_4 ring resonators.[8,9]

Several approaches have been proposed for the athermalization of ring resonators, such as active temperature control, temperature drift compensation by on-chip referencing, and the adjustment of TOC in the waveguide.[10−12] Among them, TOC adjustment is an effective and simple method.[12,13] In this waveguide, a cladding material having a negative TOC is coated onto the core having a positive TOC. When the optical mode is correctly distributed in the cladding and the core, the thermo-optic effect is counterbalanced in the waveguide and thus a temperature-independent resonator can be realized.[13−15] Among the negative TOC materials, titanium dioxide (TiO_2) has been recently investigated and applied in the athermal Si or Si_3N_4 ring resonators.[9,16,17] In these rings, the temperature-dependent wavelength shift (TDWS) can be reduced to ∼0.07 pm/°C.[9,17] However, such athermal ring resonators showed a relatively high propagation loss 3−10 dB/cm, as a consequence the Q value reported is relatively small, in the order of 10^3. Such measured Q values are much lower than the original Si or Si_3N_4 rings.[18,19] Due to the refractive index contrast between TiO_2 and the core (Si or Si_3N_4), the waveguide core in all the previous athermal ring publications must be etched to form a channel structure to obtain an adequate modal confinement in the TiO_2 cladding. In such a structure, etched-sidewall scattering becomes the primary contributor to the loss.[19,20]

In this work, we have fabricated a shallow ridge TiO_2–Si_3N_4 waveguide to realize an athermal, ultralow loss, and high-Q ring resonator. We used the Si_3N_4 as the slab layer, TiO_2 as the over cladding layer, and SiO_2/Si as the substrate. Throughout the fabrication procedures dry-etching is not necessary to obtain the designed ring structure. The dimensions of the waveguide such as the slab thickness, width, and ridge height are optimized by using the light propagation calculation method for the best optical mode confinement and the athermalization. As a result, the obtained ring resonator showed a TDWS of 0.14 pm/°C within the temperature range of 25−60 °C, a propagation loss of 0.4 dB/cm, and a Q value of 1.55×10^5 around the telecommunication wavelength.

Figure 1a shows the designed cross-section of the hybrid TiO_2–Si_3N_4 waveguide for TE mode athermal operation at

Received: November 29, 2014
Published: February 25, 2015

DOI: 10.1021/ph500450n
ACS Photonics 2015, 2, 405−409

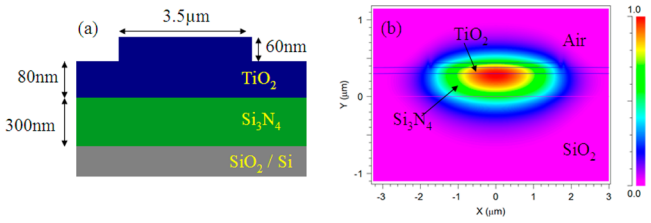

Figure 1. (a) Designed cross-section of the athermal hybrid TiO_2−Si_3N_4 waveguide, and (b) the simulated TE_0 mode distribution.

1550 nm. The height of the Si_3N_4 and TiO_2 slab are 300 and 80 nm, respectively. The TiO_2 rib has a width of 3.5 μm and a height of 60 nm. In our simulations, the waveguide supports three TE modes: TE_0, TE_1 and TE_2. However, the TE_1 and TE_2 are expected to be excited weakly in the waveguide and diminished in the microring. The optical power will be dominantly confined in the TE_0 mode, which enables a deep-resonance in the microring. Figure 1b shows the simulated TE_0 mode of the waveguide obtained by using the optical mode calculation of Rsoft, indicating a modal confinement of ~78% existing in the hybrid TiO_2−Si_3N_4 core. For comparison, we also considered an athermal single-mode TiO_2−Si_3N_4 waveguide having a rib width of 1 μm. According to the simulations, the waveguide designed in Figure 1 has a light confinement of ~10% higher than that obtained in the single mode. Such an elevated confinement property will be highly beneficial to afford a low bending loss ring, thus, providing a high-Q ring resonator. In addition, Figure 1b shows a mode diameter of 5.0 and 1.0 μm in the horizontal and vertical directions, respectively. Since this mode size is comparable to the beam size from a conventional single-mode fiber, an effective light coupling between the waveguide and the optical fiber is possible.

Generally, TDWS in a ring resonator can be expressed by using the following equation:

$$\frac{d\lambda_m}{dT} = \left(n_{eff}\cdot a_{sub} + \frac{dn_{eff}}{dT}\right)\frac{\lambda_m}{n_g} \quad (1)$$

where $d\lambda_m/dT$ is the TDWS, λ_m is the resonant wavelength, n_{eff} is the effective refractive index of the waveguide, a_{sub} is the substrate expansion coefficient, and n_g is the group index of the waveguide.[13,14] We used the measured refractive index and TOC of 2.30 and -1×10^{-4}/°C for TiO_2, 1.98 and 4×10^{-5}/°C for Si_3N_4, and 1.45 and 1×10^{-5}/°C for SiO_2. The SiO_2 substrate has an a_{sub} of 2.6×10^{-6}/°C.[14] Since the Si_3N_4 and TiO_2 thin films can be deposited precisely with the desired thicknesses, we estimated the optimal TiO_2 rib structure for the athermal condition. Figure 2a shows the calculated TDWS at different TiO_2 rib thicknesses by using eq 1. It can be observed that the TDWS is adjusted $d\lambda_m/dT = 0$ position when the thickness of the TiO_2 rib is 60 nm. We also considered the accuracy of the calculation in terms of the deviation of the materials refractive index. In our experiment, by using the prism-coupling technique, the deviation of the TiO_2 refractive index was shown to be ±0.0005. Therefore, we plotted a potential TDWS against the change of refractive index between +0.001 and −0.001. The calculation shows that the wavelength shift is only ~0.02 pm by a change in the refractive index of just 0.0005. Our estimation suggests that the true refractive index and TOC deviations should affect the TDWS, but the athermal ring resonator can be fabricated with a minimum TDWS property.

The fabrication of the hybrid TiO_2−Si_3N_4 waveguide is illustrated in Figure 3. A Si_3N_4 film with a thickness of 0.3 μm was deposited onto a SiO_2 (2 μm)/Si (500 μm) substrate using a plasma chemical vapor deposition (SAMCO PD-220) of a mixture of SiH_4, NH_3, and N_2O at 300 °C. Subsequently, an 80 nm thick TiO_2 film was RF sputtered with a deposition rate of 2 nm/min (Figure 3a). The TiO_2 film prepared under controlled temperature below 80 °C is amorphous, and it is thermally stable when the device works lower than 300 °C. Then, the microring pattern was exposed in an electron beam (EB) resist on the TiO_2 film using a 50 keV EB lithography system (ELIONIX ELS7500, Figure 3b). ZEP-520A (ZEON) was used as the resist with a thickness of 350 nm after spin coating. A 60 nm thick TiO_2 film was deposited onto the patterned resist

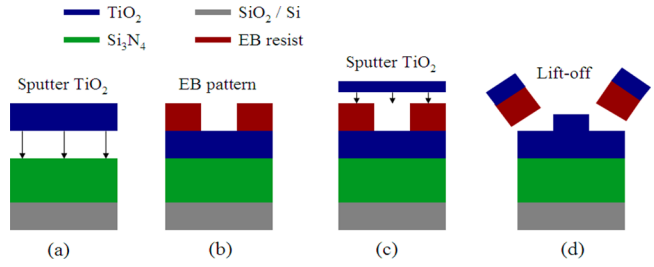

Figure 3. Fabrication process flow: (a) sputtering of a TiO_2 film (80 nm) onto a $Si_3N_4/SiO_2/Si$ wafer; (b) patterning of the microring in the EB resist; (c) sputtering of a TiO_2 film (60 nm); (d) lifting-off the EB resist.

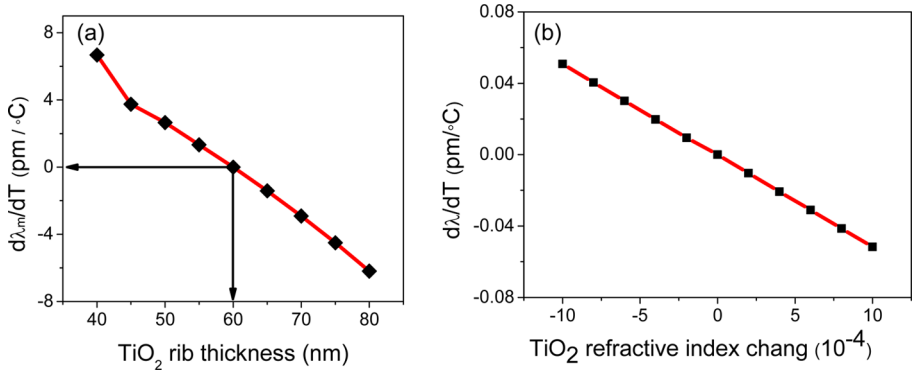

Figure 2. (a) Calculated TDWS of the waveguide at different TiO_2 rib thicknesses. (b) Change of TDWS with the possible deviation in TiO_2 refractive index.

DOI: 10.1021/ph500450n
ACS Photonics 2015, 2, 405−409

(Figure 3c). Finally, the EB resist was removed by lifting-off using *N*,*N*-dimethylacetamide as the remover and the microring structure was transformed to the 60 nm thick TiO_2 film (Figure 3d).

Figure 4a,b shows the SEM images of the hybrid TiO_2−Si_3N_4 ring resonator. The ring has a radius of 200 μm and a bus-ring gap of 400 nm. In Figure 4c,d, the cross-section indicates that the fabricated waveguide has the identical dimension to the designed one. The waveguide width of 3.50 μm and thickness of 142 nm can be clearly measured by using SEM. In the highly magnified image the slab thickness and rib height are observed to be 81 and 61 nm, respectively. The measured dimension is only 1 nm thicker than the designed structure. Such a highly precise fabrication can be attributed to (1) the controllable RF deposition of the TiO_2 film with a minimum rate of 2 nm/min; (2) EB lithography with a 10−50 nm resolution; and (3) lift-off to make a 60 nm height shallow ridge. This precise control of the waveguide dimension is preferred to achieve an optimal athermalization, which is relatively difficult to be achieve when using the dry-etching technique.

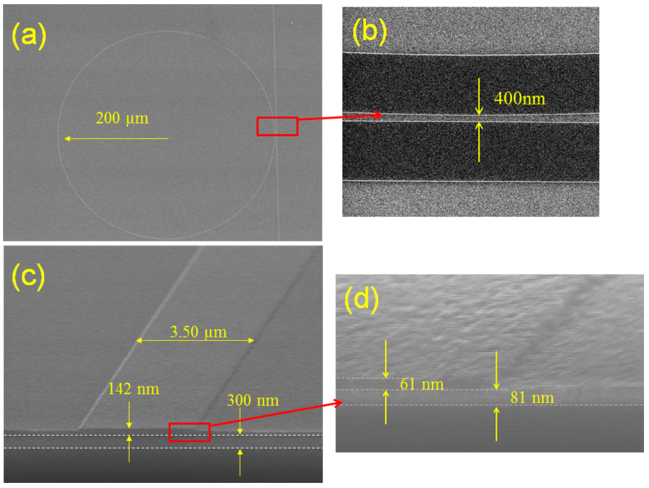

Figure 4. SEM images of the ring resonator: (a) top view, (b) bus-ring gap, (c) cross-section, and (d) zoom-in corner.

The transmission spectra of the microring were measured using an end-fire fiber coupling system. Light from a tunable laser source (TLS-510, Santec) was coupled into the waveguide in TE mode through a polarization-maintaining lensed fiber, and the wavelength was scanned with a 10 pm step. The sample was placed on a heater in order to test the TDWS between 25 and 60 °C. Finally, the output light from the waveguide was collected using another fiber and connected to a photodetector to obtain the transmission spectrum.

Figure 5a shows the transmission spectrum of the ring within the wavelength range of 1548.5−1552.0 nm at 25 °C. Four sharp resonance peaks were observed with a ∼5.5 dB extinction ratio and a relatively flat transmission spectrum between the adjacent peaks. The measured spectrum indicates that most of the optical power is in the TE_0 mode. This is consistent with our expectation that only the TE_0 mode excites in the microring. Subsequently, we focused on one resonance peak at 1549.8 nm and obtained a high resolution spectrum by scanning the laser wavelength with a 1 pm step. Using a Lorentz fit to the signals in Figure 5b, we determined that the full width at half-maximum (FWHM) of the spectrum was 0.01 nm, giving a Q-factor of 1.55×10^5. This is a record for high-Q athermal ring resonators. Although fabrication of the ring with a deeper extinction ratio is possible, we chose a high-Q operation in this work to determine the detail of the athermal properties. An enhanced resonant extinction can be obtained by improving the coupling condition between the bus and ring.

The ring is under-coupled at 1549.8 nm, so the propagation loss α in the ring, including bending loss, scattering loss and material absorption loss, can be expressed by

$$\alpha = \frac{\lambda_0}{Q_{\text{int}} \cdot R \cdot \text{FSR}} \tag{2}$$

$$Q_{\text{int}} = \frac{2Q}{1 + \sqrt{T_0}} \tag{3}$$

where λ_0 is the wavelength of one resonance peak, R is the radius of a ring, FSR is the free spectral range, and T_0 is the fraction of transmitted optical power at λ_0.[21] Using our ring having a radius of 200 μm, FSR of 0.9 nm, and T_0 of 0.27 at the λ_0 = 1549.795 nm, the propagation loss of the fabricated ring resonator was estimated to be 0.4 dB/cm. Since the modal confinement of the light dominates in the waveguide core and the sidewalls are relatively smooth, the scattering loss can be expected to be smaller than 0.05 dB/cm. In addition, TiO_2 and Si_3N_4 has a material absorption loss of ∼0.4 and <0.03 dB/cm, respectively.[20,22] Since the confinement factor of the TiO_2 layer in the waveguide is approximately 20% in Figure 1b, the material loss contribution to the waveguide should be ∼0.1 dB/cm. According to these possible estimations, we obtain a ring bending loss of 60% of the total ring propagation loss. The improvement of the bending loss, for instance by using a larger ring radius, enables the higher Q factors.

Figure 6(a) shows the fitted transmission spectra of the hybrid TiO_2−Si_3N_4 ring resonator measured at 25 and 60 °C.

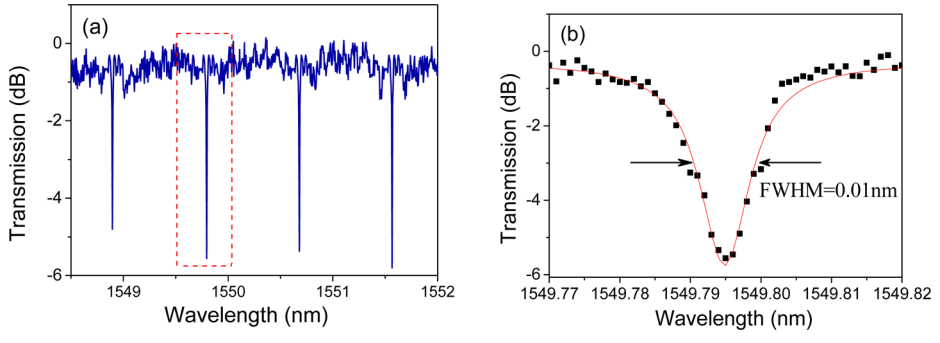

Figure 5. (a) Transmission spectrum of the ring measured at 25 °C and (b) high resolution spectrum of one resonant peak (outlined in red in (a)).

DOI: 10.1021/ph500450n
ACS Photonics 2015, 2, 405−409

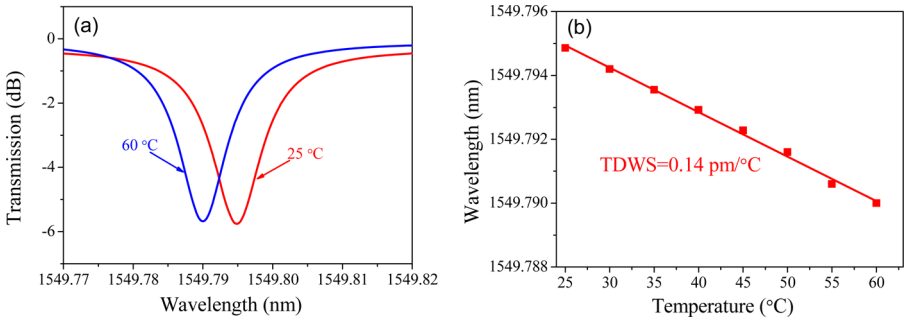

Figure 6. (a) Transmission spectra of the microring resonator at 25 and 60 °C and (b) linear fitting of the resonant wavelengths at different temperatures.

Between these two temperatures, the resonance peaks have only a 4.9 pm shift and little change in the Q values and extinctions. In Figure 6b, the linear fitting of resonance wavelengths to the various temperatures was obtained, indicating that the TDWS of the microring was 0.14 pm/°C (blue-shift). Considering the ring resonator previously reported in the $Si_3N_4/SiO_2/Si$ waveguide with a TDWS of 10 pm/°C (red-shift),[9] the hybrid TiO_2−Si_3N_4 ring resonator in this work has achieved a significantly reduced TDWS. Measured nonzero TDWS is presumably attributed to the deviations of materials, which cannot be corrected in the calculations. Since the resonance peak of the hybrid TiO_2−Si_3N_4 ring is blue-shifted at elevated temperatures, the TDWS can be further reduced by a more careful control of the TiO_2 and Si_3N_4 thickness to result in the correct optical mode balance between these two layers. The TOC of TiO_2 is constant between 18 and 120 °C and its material dispersion is small (0.001) between 1545 and 155 nm.[23,24] The TDWS will be relatively small with a 0.001 refractive index change as shown in Figure 2b, so our device can have a small TDWS within a certain range.

In summary, an athermal hybrid TiO_2−Si_3N_4 ring resonator has been designed and experimentally demonstrated. The dry etching-free fabrication technique and the shallow ridge structure enable the ring resonator to have a very small scattering loss. The Q value of the ring resonator was 1.55×10^5 and its propagation loss was 0.4 dB/cm. A TDWS of 0.14 pm/°C was measured as the result of the adjusted TO property between the Si_3N_4 slab and TiO_2 cladding. Our method should be also applicable to a range of other optical materials with a positive TOC, such as SiO_2, lithium niobate, and optical glass. Furthermore, our athermalization technique can be exploited to fabricate a range of temperature-sensitive waveguides, such as Mach−Zehnder interferometers, filters, arrayed waveguide gratings, and so on.

AUTHOR INFORMATION

Corresponding Author

*E-mail: s_yokoyama@cm.kyushu-u.ac.jp.

Notes

The authors declare no competing financial interest.

ACKNOWLEDGMENTS

This work was supported by JSPS KAKENHI Grant Nos. 26289108 and 266220712.

REFERENCES

(1) Levy, J. S.; Gondarenko, A.; Foster, M. A.; Turner-Foster, A. C.; Gaeta, A. L.; Lipson, M. CMOS-compatible multiple-wavelength oscillator for on-chip optical interconnects. *Nat. Photonics* **2010**, *4*, 37−40.

(2) Feng, S.; Lei, T.; Chen, H.; Cai, H.; Luo, X.; Poon, A. W. Silicon photonics: from a microresonator perspective. *Laser Photon. Rev.* **2012**, *6*, 145−177.

(3) Geuzebroek, D.; Klein, E.; Kelderman, H.; Baker, N.; Driessen, A. Compact wavelength-selective switch for gigabit filtering in access networks. IEEE Photon. *Technol. Lett.* **2005**, *17*, 336−338.

(4) Del'Haye, P.; Schliesser, A.; Arcizet, O.; Wilken, T.; Holzwarth, R.; Kippenberg, T. J. Optical frequency comb generation from a monolithic microresonator. *Nature* **2007**, *450*, 1214−1217.

(5) Vollmer, F.; Braun, D.; Libchaber, A.; Khoshsima, M.; Teraoka, I.; Arnold, S. Protein detection by optical shift of a resonant microcavity. *Appl. Phys. Lett.* **2002**, *80*, 4057−4059.

(6) Carlborg, C. F.; Gylfason, K. B.; Kázmierczak, A.; Dortu, F.; Bãnuls, M. J.; Catala, A. M.; Kresbach, G. M.; Sohlstrom, H.; Moh, T.; Vivien, L.; Popplewell, J.; Ronan, G.; Barrios, C. A.; Stemme, G.; van der Wijngaart, W. A packaged optical slot-waveguide ring resonator sensor array for multiplex label-free assays in labs-on-chips. *Lab Chip* **2010**, *10*, 281−290.

(7) Levy, J. S.; Foster, M. A.; Gaeta, A. L.; Lipson, M. Harmonic generation in silicon nitride ring resonators. *Opt. Express* **2011**, *19*, 11415−11421.

(8) Gylfason, K. B.; Carlborg, C. F.; Kaźmierczak, A.; Dortu, F.; Sohlström, H.; Vivien, L.; Barrios, C. A.; van der Wijngaart, W.; Stemme, G. On-chip temperature compensation in an integrated slot-waveguide ring resonator refractive index sensor array. *Opt. Express* **2010**, *18*, 3226−3237.

(9) Qiu, F.; Spring, A. M.; Yu, F.; Yokoyama, S. Complementary metal−oxide−semiconductor compatible athermal silicon nitride/titanium dioxide hybrid micro-ring resonators. *Appl. Phys. Lett.* **2013**, *102*, 051106.

(10) Qiu, C.; Shu, J.; Li, Z.; Zhang, X.; Xu, Q. Wavelength tracking with thermally controlled silicon resonators. *Opt. Express* **2011**, *19*, 5143−5148.

(11) Guha, B.; Kyotoku, B.; Lipson, M. CMOS-compatible athermal silicon microring resonators. *Opt. Express* **2010**, *18*, 3487−3493.

(12) Teng, J.; Dumon, P.; Bogaerts, W.; Zhang, H.; Jian, X.; Han, X.; Zhao, M.; Morthier, G.; Baets, R. Athermal silicon-on-insulator ring resonators by overlaying a polymer cladding on narrowed waveguides. *Opt. Express* **2009**, *17*, 14627−14633.

(13) Padmaraju, K.; Bergman, K. Resolving the thermal challenges for silicon microring resonator devices. *Nanophotonics* **2013**, *2*, 1−14.

(14) Qiu, F.; Yu, F.; Spring, A. M.; Yokoyama, S. Athermal silicon nitride ring resonator by photobleaching of Disperse Red 1-doped poly(methyl methacrylate) polymer. *Opt. Lett.* **2012**, *37*, 4086−4088.

(15) Kokubun, Y.; Yoneda, S.; Tanaka, H. Temperature-independent narrowband optical filter at 1.31 μm wavelength by an athermal waveguide. *Electron. Lett.* **1996**, *32*, 1998−2000.

(16) Bovington, J.; Wu, R.; Cheng, K. T.; Bowers, J. E. Thermal stress implications in athermal TiO_2 waveguides on a silicon substrate. *Opt. Express* **2014**, *22*, 661−666.

DOI: 10.1021/ph500450n
ACS Photonics 2015, 2, 405−409

(17) Guha, B.; Cardenas, J.; Lipson, M. Athermal silicon microring resonators with titanium oxide cladding. *Opt. Express* **2013**, *21*, 26557−26563.
(18) Baehr-Jones, T.; Hochberg, M.; Walker, C.; Scherer, A. High-Q ring resonators in thin silicon-on-insulator. *Appl. Phys. Lett.* **2004**, *85*, 3346−3347.
(19) Bauters, J. F.; Heck, M. J. R.; John, D.; Dai, D.; Tien, M.-C.; Barton, J. S.; Leinse, A.; Heideman, R. G.; Blumenthal, D. J.; Bowers, J. E. Ultra-low-loss high-aspect-ratio Si_3N_4 waveguides. *Opt. Express* **2011**, *19*, 3163−3174.
(20) Tien, M.-C.; Bauters, J. F.; Heck, M. J. R.; Spencer, D. T.; Blumenthal, D. J.; Bowers, J. E. Ultra-high quality factor planar Si_3N_4 ring resonators on Si substrates. *Opt. Express* **2011**, *19*, 13551−13556.
(21) Rabiei, P.; Steier, W. H.; Zhang, C.; Dalton, L. R. Polymer micro-ring filters and modulators. *J. Lightwave Technol.* **2002**, *20*, 1968−1975.
(22) Bradley, J. D. B.; Evans, C. C.; Choy, J. T.; Reshef, O.; Deotare, P. B.; Parsy, F.; Phillips, K. C.; Loncar, M.; Mazur, E. Submicrometer-wide amorphous and polycrystalline anatase TiO_2 waveguides for microphotonic devices. *Opt. Express* **2012**, *20*, 23821−23831.
(23) Gulsen, G.; Inci, M. N. Thermal optical properties of TiO_2 films. *Opt. Mater.* **2002**, *18*, 373−381.
(24) Furuhashi, M.; Fujiwara, M.; Ohshiro, T.; Tsutsui, M.; Matsubara, K.; Taniguchi, M.; Takeuchi, S.; Kawai, T. Development of microfabricated TiO_2 channel waveguides. *AIP Adv.* **2011**, *1*, 1−5.

DOI: 10.1021/ph500450n
ACS Photonics 2015, 2, 405−409